# EXPERIMENTAL RESULTS WITH A SIMPLIFIED MODEL BASED WAVE FILTER WITH INERTIAL SENSOR FEEDBACK FOR SURFACE VESSELS

**Karl-Petter Lindegaard*, Bjørnar Vik and Thor I. Fossen**

Department of Engineering Cybernetics
Norwegian University of Science and Technology, N-7491 Trondheim, Norway
E-mail : kpl,bvik,tif@itk.ntnu.no
Fax : (+47) 73594399

**Keywords:** Marine vehicle control, inertial navigation, observers, asymptotic stability

## Abstract

A new model based observer for surface vessels which incorporates inertial measurements is proposed and analyzed. The purpose of this extension is to pave the way for taking advantage of measured accelerations and angular velocities in positioning operations of marine craft. The proposed filter is easy to tune and handles unsynchronized measurements better than previous designs. Exposing a model ship exposed to irregular waves while performing a dynamic positioning operation illustrates performance.

## 1 Introduction

Dynamic positioning (DP) of surface vessels, that is to make a vessel maintain its desired position despite the environmental disturbances acting upon it, is a field of control engineering that has received the attraction of many researchers. A large variety of solutions has been proposed. A fundamental part of all marine vessel control systems is the filter used to filter out the rapidly varying dynamics of the first order wave induced motion. The first order wave loads force the vessel to oscillate with a resonance frequency close to the mean of the incoming waves. For two reasons it is undesirable to attenuate this resonant motion: First, the first order forces have a zero mean and secondly, the frequency is so high that trying to cancel out the induced motion will only lead to thruster modulation and, as a result, reduced thruster life time. Consequently, it is of paramount importance to filter out frequency components around the peak frequency of the wave spectrum and concentrate on counteracting the low frequency (LF) disturbances instead. Typically wind, ocean current and higher order nonlinear wave effects (constant drift and LF resonant motion) belong to this category.

The most industrially significant contribution to solving the DP problem was probably the application of LQG-control [2] in the mid-1970's. The first order wave induced motion was treated as measurement noise and a Kalman filter was used to reconstruct the system's LF states such as velocities and positions based on position measurements. Today, over 25 years later, most DP systems still only utilize position measurements for feedback although wind feedforward is frequently used to better keep up with gusting winds. The trend has been to employ more advanced and complex control theory in the search for better

*Supported by The Research Council of Norway through the Stategic University Program on Marine Cybernetics and ABB AS, Oslo, Norway.

performance and robustness.

Two important facts remain though. It is not apparent that complex control theory leads to better performance than for instance LQG or even PID-control. A poorly tuned controller is still a poorly tuned controller regardless of the underlying philosophy. Secondly, a ship can be (roughly) described by a first order low-pass filter and stabilizing such dissipative systems can be done with a minimum of engineering effort.

A completely different approach is to put forward a new set of terms for how a DP system can be designed. It is important to raise questions like how new technology may contribute to improving the positioning performance (safety) and to decrease the operational costs. One such concept is to estimate the unmeasurable slowly varying drift forces due to second order wave loads, so called wave feedforward [1]. Another approach is to employ high precision inertial sensor technology in order to extend existing output-feedback designs [5].

In a previous paper [5] we introduced a model based observer with wave filtering capabilities for surface vessels at low speed. Although this observer was the first model based integrated design that could incorporate partial velocity and acceleration measurements, there are two reasons why this design is unsuited from an industrial point of view. At the core of these problems is the suggested model of first order wave induced motion:

1. The tuning procedure is much more complicated when velocity and/or acceleration measurements are included compared to the pole placement strategy used for position measurements. This is due to the fact that in the general case the observer gains enter non-affinely in the expressions describing the eigenvalue of the observer error-dynamics. One solution is to solve an algebraic Riccati equation (Kalman gains or $\mathcal{H}_\infty$-filtering techniques) either a priori or on-line, but having complete control of the notch-effects is almost impossible. As a consequence, it is very likely that the time spent tuning the DP system during sea-trials increases.

2. A common wave model for all state derivatives could be fatal for stability of the combined wave motion model if the individual measurements are out of synchronization with respect to each other. This occurs e.g. if the time-delays from the sensor system components are different.

In this paper we propose a model based observer where the wave models are considered separately for position, velocity and acceleration measurements. The main idea is that wave induced acceleration is "uncorrelated" with the induced velocity, an assumption that is motivated more from engineering experience rather than physics.

In the next section a low-speed model of a vessel is presented together with the distributed wave models. The observer design and stability analysis is covered in section three. In section four we suggest a tuning rule based on the filter's desired frequency response and the needed $g$-compensator is described in section five. Experiments with a model ship exposed to irregular waves is reported in section six and some concluding remarks are drawn in section seven.

## 2 Modeling

### 2.1 Vessel and Environment Model

We consider the dynamics of a vessel in three degrees of freedom, the horizontal plane, and we choose to express the model in the Earth- and body-fixed coordinate frames. The body-fixed frame coincides with the principal axes of the vessel and it is rotated an angle $\psi_y$ with respect to the Earth-fixed frame. This transformation of coordinates is represented by the orthogonal rotation matrix

$$R(\alpha) = \begin{bmatrix} \cos\alpha & -\sin\alpha & 0 \\ \sin\alpha & \cos\alpha & 0 \\ 0 & 0 & 1 \end{bmatrix} \qquad (1)$$

and its time-derivative is $\dot{R}(\alpha) \triangleq \frac{d}{dt}(R(\alpha)) = \dot{\alpha}SR(\alpha)$ where the skew-symmetric $S$ is

$$S = \begin{bmatrix} 0 & -1 & 0 \\ 1 & 0 & 0 \\ 0 & 0 & 0 \end{bmatrix} \tag{2}$$

In [5] we used the concept of commutating matrices to simplify the observer design, a tool that is going to be used here as well.

**Property 1** *A matrix $A \in \mathbb{R}^{3\times 3}$ is said to* commute *with the rotation $R(\alpha)$ if*

$$AR(\alpha) = R(\alpha)A \tag{3}$$

Let $\eta = [x, y, \psi]^T$ denote the LF position where $x$ and $y$ are the North and East positions respectively, and $\psi$ is the LF heading. Define $\nu = [u, v, r]^T$ as the LF body-fixed velocities, i.e. surge, sway and yaw. It is assumed that all three positions are available for feedback and that $n_{y_2} \geq 0$ velocities and $n_{y_3} \geq 0$ accelerations are available.

The system model is assumed to satisfy:

**A1** The orientation angle between the Earth-fixed and body-fixed frame is the measured heading $\psi_y$ such that:

$$\begin{aligned} \dot{p}_w &= A_{pw}p_w + E_{pw}w_{pw} && (4)\\ \dot{v}_w &= A_{vw}v_w + E_{vw}w_{vw} && (5)\\ \dot{a}_w &= A_{aw}a_w + E_{aw}w_{aw} && (6)\\ \dot{\eta} &= R(\psi_y)\nu && (7)\\ \dot{b} &= -T_b^{-1}b + E_b w_b && (8)\\ M\dot{\nu} &= -GR^T(\psi_y)\eta - D\nu \\ &\quad +\tau + R^T(\psi_y)b && (9) \end{aligned}$$

where $b \in \mathbb{R}^3$ is an unknown bias force due to LF environmental loads, $\tau \in \mathbb{R}^3$ is the applied thruster force, $M = M^T > 0$ is the mass, $D \in \mathbb{R}^{3\times 3}$ contains linear damping coefficients and $G \in \mathbb{R}^{3\times 3}$ describes possible mooring forces. The bias forces $b$ are modelled as Markov processes with a positive semi-definite diagonal matrix $T_b^{-1} \in \mathbb{R}^{3\times 3}$ of time constants. The order of each wave model number is arbitrary, but it is recommended to keep the order fairly low. Second or fourth order linear models are sufficient. Let $m_p$, $m_v$, $m_a$ denote the order of the position, velocity and acceleration wave models respectively. Then $p_w \in \mathbb{R}^{3m_p}$,$v_w \in \mathbb{R}^{n_{y_2}\cdot m_v}$, $a_w \in \mathbb{R}^{n_{y_3}\cdot m_a}$ describe the first order wave-induced positions, velocities and accelerations respectively. $A_{pw} \in \mathbb{R}^{3m_p\times 3m_p}$, $A_{vw} \in \mathbb{R}^{n_{y_2}\cdot m_v\times n_{y_2}\cdot m_v}$, $A_w \in \mathbb{R}^{n_{y_3}\cdot m_a\times n_{y_3}\cdot m_a}$ are assumed Hurwitz and describes the first order wave induced motion. The wave and bias models are driven by disturbances of appropriate dimensions. A more detailed model description in given in [4].

In order to make use of the commutation properties, we have to assume

**A2** The bias time constant matrix $T_b$ and each $3 \times 3$ sub-block of $A_{pw}$ satisfies Property 1.

Collect the Earth-fixed states in $x_1 \in \mathbb{R}^{6+3m_p}$ and the body-fixed in $x_2 \in \mathbb{R}^{3+n_{y_2}\cdot m_v+n_{y_3}\cdot m_a}$

$$\begin{aligned} x_1 &= \begin{bmatrix} p_w^T & \eta^T & b^T \end{bmatrix}^T && (10)\\ x_2 &= \begin{bmatrix} v_w^T & a_w^T & \nu^T \end{bmatrix}^T && (11) \end{aligned}$$

Let $n$ denote the dimension of $x = [x_1^T, x_2^T]^T$ and define the block diagonal transformation matrix $T : \mathbb{R} \to \mathbb{R}^{n\times n}$

$$\begin{aligned} T(\psi_y) = \mathrm{Diag}(&R^T\left(\psi_y\right), ... \\ &, R^T\left(\psi_y\right), I_{3+n_{y_2}\cdot m_v+n_{y_3}\cdot m_a}) \end{aligned} \tag{12}$$

On compact form using Assumption A2 and $w = [w_{pw}^T, w_b^T, w_{vw}^T, w_{aw}^T]^T$ we get

$$\dot{x} = T^T(\psi_y)AT(\psi_y)x + B\tau + Ew \tag{13}$$

where the parameters $A$ have been separated from the rotation $R(\psi_y)$. Using $\bar{M} = M^{-1}$ the model parameters in (13) are

$$A = \begin{bmatrix} A_{pw} & 0 & 0 & 0 & 0 & 0 \\ 0 & 0 & 0 & 0 & 0 & I \\ 0 & 0 & -T_b^{-1} & 0 & 0 & 0 \\ 0 & 0 & 0 & A_{vw} & 0 & 0 \\ 0 & 0 & 0 & 0 & A_{aw} & 0 \\ 0 & -\bar{M}G & \bar{M} & 0 & 0 & -\bar{M}D \end{bmatrix} \tag{14}$$

$$B = \begin{bmatrix} 0 \\ 0 \\ 0 \\ 0 \\ 0 \\ \bar{M} \end{bmatrix}, \quad E = \begin{bmatrix} E_{pw} & 0 & 0 & 0 \\ 0 & 0 & 0 & 0 \\ 0 & E_b & 0 & 0 \\ 0 & 0 & E_{vw} & 0 \\ 0 & 0 & 0 & E_{aw} \\ 0 & 0 & 0 & 0 \end{bmatrix} \tag{15}$$

### 2.2 Measurements

The number velocity and acceleration measurements available are denoted $n_{y_2}$ and $n_{y_3}$ respectively. Let $y_1 \in \mathbb{R}^3$, $y_2 \in \mathbb{R}^{n_{y_2}}$ and $y_3 \in \mathbb{R}^{n_{y_3}}$ describe the position, velocity and acceleration measurement vectors. We define the measurements as

$$\begin{aligned} y_1 &= \eta + C_{pw} p_w & (16) \\ y_2 &= \Upsilon_2 \nu + C_{vw} v_w & (17) \\ y_3 &= \Upsilon_3 \dot{\nu} + C_{aw} a_w & (18) \end{aligned}$$

where, $\Upsilon_2$ and $\Upsilon_3$ are projections isolating the components of the LF-model that are actually measured. Written compactly,

$$y = C_y(\psi_y) x + D_y \tau \tag{19}$$

where

$$C_y(\psi_y) = \begin{bmatrix} C_{pw} & I & 0 \\ \Upsilon_2 C_v R^T & 0 & 0 \\ 0 & -\Upsilon_3 M^{-1} G R^T & -\Upsilon_3 R^T \\ 0 & 0 & 0 \\ \Upsilon_2 & C_{vw} & 0 \\ -\Upsilon_3 M^{-1} D & 0 & C_{aw} \end{bmatrix}$$

$$D_y = \begin{bmatrix} 0 & 0 & M^{-T} \Upsilon_3^T \end{bmatrix}^T \tag{20}$$

Physically however, it should be pointed out that the LF linear accelerations that are being measured is not $\dot{\nu}$ as claimed in (18) but $\ddot{\eta} \neq \dot{\nu}$ when the Earth-fixed frame is considered as being the inertial frame. More specifically, considering the LF dynamics

$$y_{3,lf} = \ddot{\eta} = \dot{\psi}_y S R(\psi_y) \nu + R(\psi_y) \dot{\nu} \tag{21}$$

which means that (18) is approximately correct for small angular rates. For large angular rates, however, an auxiliary pre-processor should be used to compensate for the Coriolis effect $\dot{\psi}_y S R(\psi_y) \nu$. The need for an external processing unit will in fact always be there as discussed in Section 5.

## 3 Observer Design

By duplicating the model dynamics and introducing a low-pass filter in order to achieve a certain roll-off effect, see (46), the following model based observer is proposed

$$\dot{a}_f = T_f^{-1} \left( -a_f + \tilde{y}_3 \right) \tag{22}$$

$$\dot{\hat{x}} = T^T(\psi_y) A T(\psi_y) \hat{x} + B\tau + K(\psi_y) \tilde{y} + K_f a_f \tag{23}$$

and its estimated output is

$$\hat{y} = C_y(\psi_y) \hat{x} + D_y \tau \tag{24}$$

and hence when the estimation error is $\tilde{x} = x - \hat{x}$, the output error is $\tilde{y} = C_y(\psi_y) \tilde{x}$.

A very neat selection of observer gain matrices $K(\psi_y)$ and $K_f$ that reduces interconnections is

$$K(\psi_y) = \begin{bmatrix} K_{11} & 0 & 0 \\ K_{21} & 0 & 0 \\ K_{31} & 0 & 0 \\ 0 & K_{42} & 0 \\ 0 & 0 & K_{53} \\ K_{61} R^T(\psi_y) & K_{62} & 0 \end{bmatrix} \tag{25}$$

$$K_f = \begin{bmatrix} 0 & 0 & 0 & 0 & 0 & K_a^T \end{bmatrix}^T \tag{26}$$

A schematic drawing of this observer, without bias estimation, is given in Figure 1.

### 3.1 Stability Analysis

If each and every $3 \times 3$ block of $K_{11}$, $K_{21}$ and $K_{31}$ commute with the rotation $R(\psi_y)$, the rotations can be separated from the parameters. The observer error-dynamics can hence be rewritten on the compact form

$$\begin{aligned} \dot{\tilde{x}} &= T^T(\psi_y) A_o T(\psi_y) \tilde{x} + K_f a_f + E_e w & (27) \\ \dot{a}_f &= -T_f^{-1} a_f + T_f^{-1} C_3 T(\psi_y) \tilde{x} & (28) \end{aligned}$$

$$A_o = \begin{bmatrix} A_{11} & A_{12} \\ A_{21} & A_{22} \end{bmatrix} \tag{29}$$

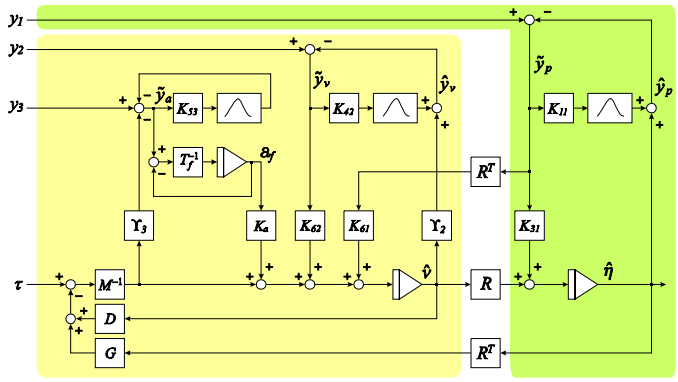


Figure 1: Observer with first order cut-off filter for acceleration. Bias estimation is not shown.

$$A_{11} = \begin{bmatrix} A_{pw} - K_{11}C_{pw} & -K_{11} & 0 \\ -K_{21}C_{pw} & -K_{21} & 0 \\ -K_{31}C_{pw} & -K_{31} & -T_b^{-1} \end{bmatrix} \quad (30)$$

$$A_{12} = \begin{bmatrix} 0 & 0 & 0 \\ 0 & 0 & I \\ 0 & 0 & 0 \end{bmatrix} \quad (31)$$

$$A_{21} = \begin{bmatrix} 0 & 0 & 0 \\ 0 & 0 & 0 \\ -K_{61}C_{pw} & -M^{-1}G - K_{61} & M^{-1} \end{bmatrix} \quad (32)$$

$$A_{22} = \begin{bmatrix} A_{vw} - K_{42}C_{vw} & 0 & -K_{42}\Upsilon_2 \\ 0 & A_{aw} - K_{53}C_{aw} & -K_{53}\Upsilon_3 \\ -K_{62}C_{vw} & 0 & -M^{-1}D - K_{62}\Upsilon_2 \end{bmatrix}$$

$$C_3 = \begin{bmatrix} 0 & -\Upsilon_3 M^{-1}G & \Upsilon_3 M^{-1} \\ & & -\Upsilon_3 M^{-1}D \quad 0 \quad C_{aw} \end{bmatrix} \quad (33)$$

Stacking (27)-(28) together into $z \in R^{n_z}$, more specifically $z = [\tilde{x}^T, a_f^T]^T$, we then get

$$\dot{z} = T_z^T(\psi_y) A_z T_z(\psi_y) z + E_z w \quad (34)$$

where $T_z = \mathrm{Diag}(T, I_{n_{y_3}})$ and

$$A_z = \begin{bmatrix} A_o & K_f \\ T_f^{-1}C_3 & -T_f^{-1} \end{bmatrix} \quad , \quad E_z = \begin{bmatrix} E_e \\ 0 \end{bmatrix} \quad (35)$$

We now state a robustness-like theorem for stability of this filter. The limiting factor is the yaw rate $\dot{\psi}_y = r_y$ and we could just as well employ the result from [5], that is using a $P$-matrix in a quadratic Lyapunov function of a certain structure that commutes with $T_z(\psi_y)$. Because the upper bound on $|r_y(t)|$ will be larger than the physical limit, we assign an arbitrary $P$. The advantage of an arbitrarily selected $P$ is that there are no longer any restrictions on the selection of cross-terms. As a consequence we could have let $T_b \to \infty$, then the bias is modelled as an open integrator and we obtain true integral action.

Before we state the theorem we need to introduce a skew-symmetric matrix $S_z$ that appears when the rotation $T_z(\psi_y)$ is differentiated.

$$\dot{T}_z \triangleq \frac{d}{dt}\left(T_z(\psi_y)\right) = \dot{\psi}_y S_z T_z(\psi_y) = \dot{\psi}_y T_z(\psi_y) S_z \quad (36)$$

In our case $S_z = \mathrm{Diag}(S^T, ..., S^T, 0_{n_z-12 x n_z-12})$ where $S$ is given by (2).

**Theorem 2** *The observer error dynamics (34) is exponentially stable for small $|r_y(t)| < r_{\max}$ (ULES) if and only if $A_z$ is Hurwitz. Suppose an $r_{\max} > 0$ is explicitly given, then (34) is uniformly globally exponentially stable (UGES) if there exists a matrix $P = P^T > 0$ such that the following two LMIs are feasible for some $\varepsilon > 0$*

$$\begin{aligned} PA_z + A_z^T P + \varepsilon I &\leq r_{\max}\left(PS_z + S_z^T P\right) \\ PA_z + A_z^T P + \varepsilon I &\leq -r_{\max}\left(PS_z + S_z^T P\right) \end{aligned} \quad (37)$$

Notice that stability can be characterized without dealing with the rotations $T_z(\psi_y)$. However, there is a bound on the rotation rate $r_{\max}$ making the observer due to observability semi-globally exponentially stable.

**Proof.** Use the non-singular rotation $T_z(\psi_y)$ as a mapping $\xi = T_z z$. Then,

$$\begin{aligned} \dot{\xi} &= \dot{T}_z z + T_z \dot{z} \\ &= \dot{\psi}_y S_z T_z z + T_z T_z^T A_z T_z z \\ &= \left(A_z + \dot{\psi}_y S_z\right)\xi \end{aligned} \quad (38)$$

Consider the Lyapunov function $V = \xi^T P \xi$

$$\begin{aligned}\dot{V} &= \xi^T \left(P A_z + A_z^T P\right) \xi \\ &\quad + \dot{\psi}_y \xi^T \left(P S_z + S_z^T P\right) \xi \end{aligned} \tag{39}$$

Since $\dot{V}$ is linear in $\dot{\psi}_y$ for fixed $P$ and $\xi$ it is also convex and it suffices to verify that $\dot{V} < 0$ at the boundaries of $\dot{\psi}_y$, namely $\pm r_{\max}$ since $-r_{\max} \leq \dot{\psi}_y \leq r_{\max}$ by assumption. We therefore have to make sure that

$$\dot{V}_1 = \dot{V}\Big|_{\dot{\psi}_y = r_{\max}} < 0 \tag{40}$$

$$\dot{V}_2 = \dot{V}\Big|_{\dot{\psi}_y = -r_{\max}} < 0 \tag{41}$$

Inserting the LMIs from (37) we get for $k = 1, 2$

$$\dot{V}_k \leq -\varepsilon I \tag{42}$$

For small enough $r_{\max}$, there will always exist an $\varepsilon > 0$ if and only if $A_z$ is Hurwitz. ■

This result could also be proven by the circle criterion, but the maximum allowable $r_{\max}$ is likely to be smaller due to the required SPR-property.

Notice that stability can be proven even though the bias time constant $T_b$ is infinite, that is $T_b^{-1} = 0$. The passive design [3] and our previous version [5] need $T_b^{-1} > 0$ and if $T_b^{-1}$ is indeed positive definite, *global* exponential stability, for all $r_{\max} > 0$ that is, of the observer error can be verified using a $P$-matrix of a certain structure [5].

# 4 Observer Tuning

In this section we suggest models for the first order wave loads and then we suggest tuning rules that based on those models generate the desired frequency response between the measurements and the LF estimates.

For position and velocity measurements, $i = p, v, a$ a cascade of second order linear systems

$$A_{iw} = \begin{bmatrix} 0 & I \\ -\Omega_i & -\Lambda_i \end{bmatrix} \quad , \quad C_{iw} = \begin{bmatrix} 0 & I \end{bmatrix} \tag{43}$$

can be used to represent the wave induced motion and thereby obtain the desired wave filtering capability. Treat each DOF separated from the others by setting

$$\Omega_i = \text{diag}(\omega_{i,1}^2, ..., \omega_{i,n_{y_i}}^2) \tag{44}$$

$$\Lambda_i = \text{diag}(2\zeta_{i,1}\omega_{i,1}, ..., 2\zeta_{i,n_{y_i}}\omega_{i,n_{y_i}}) \tag{45}$$

where $\omega_{i,k} > 0$ is the resonance frequency and $\zeta_{i,k} > 0$ is the relative damping factor which determines the width of the spectrum.

Depending on the number $p_i = \frac{m_i}{2}$, where $i = p, v, a$ of second order models in cascade, the desired transfer function between any measurement and the LF estimate is

$$h_d(s) = \omega_{c,k} \frac{\left(s^2 + 2\zeta_{i,k}\omega_{i,k}s + \omega_{i,k}^2\right)^{p_i}}{\left(s^2 + 2\delta_{i,k}\zeta_{i,k}\omega_{i,k}s + \omega_{i,k}^2\right)^{p_i} (\omega_{c,k} + s)} \tag{46}$$

which is a notch-filter, with center frequency at $\omega_{i,k}$, the wave model resonance, and notch "width" given by $\delta_{i,k} \geq 1$, in series with a low-pass filter that guarantees a certain roll-off for frequencies larger than $\omega_{c,k}$. In order to achieve good performance the roll-off frequency should be larger than the resonance frequency of the notch-filter, that is $\omega_{c,k} \geq \omega_{i,k}$.

## 4.1 Wave Model Gains

We apply exactly the same pole-placement technique to find observer gains for position and velocity innovation. If we were dealing with second order wave models, the tuning rules from [4] apply. However, due to the increasing power of the wave frequency components in the velocity and acceleration signal, we suggest using a fourth order wave model, at least for acceleration, in order to achieve satisfactory wave filtering capabilities. We were in fact unable to get good results for acceleration using second order models. Below, we therefore present the extension of [4] to fourth order models.

Consider the surge dynamics being updated from position measurements. We aim to find the elements to put in $K_{11}$ and $K_{31}$ in order to create the desired notch and roll-off $h_d(s)$ in (46)

$$\frac{\hat{\eta}}{y_1}(s) = h_d(s) \tag{47}$$

This can be obtained one degree of freedom at the time by defining $\alpha_{p,i} = \omega_{p,i}^2 > 0$ and $\beta_{p,i} = 2\zeta_{p,i}\omega_{p,i} > 0$ and letting

$$A_{pw,1} = \begin{bmatrix} 0 & 1 & 0 & 0 \\ -\alpha_{p,i} & -\beta_{p,i} & 0 & 1 \\ 0 & 0 & 0 & 1 \\ 0 & 0 & -\alpha_{p,i} & -\beta_{p,i} \end{bmatrix} \quad (48)$$

$$\bar{C}_{pw,1} = \begin{bmatrix} 1 & 0 & 0 & 0 \end{bmatrix} \quad (49)$$

and picking observer gains according to

$$K_{11,1} = L_1^{-1} c_1 \quad (50)$$

$$K_{31,1} = \omega_{c,1} \quad (51)$$

where

$$L_i = \begin{bmatrix} 1 & 0 & 0 & 0 \\ 2\beta_{p,i} & 1 & 0 & 0 \\ \alpha_{p,i} + \beta_{p,i}^2 & \beta_{p,i} & 0 & 1 \\ \beta_{p,i} & 1 & -1 & 0 \end{bmatrix} \quad (52)$$

$$c_i = \begin{bmatrix} 2\beta_{p,i}\left(\delta_{p,i} - 1\right) \\ \beta_{p,i}^2\left(\delta_{p,i}^2 - 1\right) + 2\beta_{p,i}\left(\delta_{p,i} - 1\right)\omega_{c,i} \\ \alpha_{p,i}\beta_{p,i}\left(\delta_{p,i} - 1\right) + \beta_{p,i}^2\left(\delta_{p,i}^2 - 1\right)\omega_{c,i} \\ 2\beta_{p,i}\left(\delta_{p,i} - 1\right)\omega_{c,i} \end{bmatrix} \quad (53)$$

ensures that the specified notch-effect and roll-off is indeed acquired. The gains $K_{31}$ and $K_{61}$, the gains from position innovation which update the bias and LF velocity, can be selected freely as long as $A_z$ remains Hurwitz.

The exact same approach can be applied to assign values to $K_{42}$, $K_{62}$ in order to obtain a notch-effect for the velocity measurements.

### 4.2 Acceleration Gains

The acceleration part of the filter possesses another feature as well. Measuring the acceleration could be regarded as an alternative to using a model based observer because the model actually estimates the acceleration while an accelerometer measures it. The gain $K_f$ serves as a weight factor determining how much emphasis we should put on the model. When $K_f = 0$ we choose not to utilize acceleration feedback to update the filter at all and when $K_f = 1$, the LF model description is completely disregarded for low frequencies.

The low-pass filter between acceleration innovation $\tilde{y}_3$ and $\dot{\hat{\nu}}$ takes care of the roll-off. The filter constants $T_f$ should therefore be selected as

$$T_f^{-1} = \mathrm{diag}(\omega_{c,1}, ..., \omega_{c,n_{y_3}}) \quad (54)$$

Next, to obtain the desired notch-filtering around the resonance frequency, select

$$K_{53} = \begin{bmatrix} 0 \\ \mathrm{diag}(\delta_{a,1}, ..., \delta_{a,n_{y_3}}) \end{bmatrix} \quad (55)$$

## 5 Accelerometer Measurements

Accurate measurements of surge and sway acceleration require good roll and pitch measurements. This is due to the fact that an accelerometer cannot distinguish between gravity and acceleration. Thus, even small roll and pitch angles will lead to gravity components in the acceleration measurements along the surge and sway axes. When the angular motion of a ship is periodic, gyros can be used to measure the dynamic motion of the ship, while the accelerometers can be used to measure the LF part of the angular motion.

Assuming that the accelerometers are at rest, we can write:

$$f_{\mathrm{imu}} = -R_n^b g^n \quad (56)$$

where $f_{\mathrm{imu}} \in \mathbb{R}^3$ is measured by the accelerometers, $R_n^b \in SO3$ is the rotation matrix from the local frame to the body frame, and $g^n \in \mathbb{R}^3$ is the local frame gravity vector. On component form this is written:

$$\begin{bmatrix} f_x \\ f_y \\ f_z \end{bmatrix} = -\begin{bmatrix} -\sin\theta \\ \cos\theta\sin\phi \\ \cos\theta\cos\phi \end{bmatrix} g \quad (57)$$

Roll and pitch angles can be found from:

$$\phi = \arctan(\frac{f_y}{f_z}) \quad (58)$$

$$\theta = \arctan(\frac{f_x}{\sqrt{f_z^2 + f_y^2}}) \quad (59)$$

By assuming that the roll and pitch errors are small, the following expressions are obtained:

$$\delta\phi \approx \frac{\delta f_y}{g} \quad , \quad \delta\theta \approx \frac{\delta f_x}{g} \quad (60)$$

where $\delta\phi$ and $\delta\theta$ are the roll and pitch errors, and $\delta f_y$ and $\delta f_x$ are $y$ and $x$ axes accelerometer errors. It can be seen that a 1 m$g$ accelerometer error gives a roll and pitch static accuracy of 1 mrad $\approx$ 0.06 degrees. In order to measure dynamic roll and pitch accurately, a filter must be designed that integrates gyro and accelerometer measurements. This is often referred to as a vertical reference unit (VRU) and such can be implemented using a Kalman filter or an observer. In this work, we have used the observer developed in [7]. The observer is written:

$$\dot{\hat{q}} = \frac{1}{2}T_{\hat{q}}(\hat{q})R(\tilde{q})\left[\omega_{\text{imu}} + \hat{b}_{\text{gyro}} + K_1\tilde{\varepsilon_q}\,\text{sgn}(\tilde{\eta}_q)\right] - \frac{1}{2}\Xi(\hat{q})\omega_{in}^n \tag{61}$$

$$\dot{\hat{b}}_{\text{gyro}} = -T_{\text{gyro}}^{-1}\hat{b}_{\text{gyro}} + \frac{1}{2}K_2\tilde{\varepsilon}_q\,\text{sgn}(\tilde{\eta}_q) \tag{62}$$

where $\hat{q} \in \mathbb{H}$, is the four element unit quaternion

$$\mathbb{H} = \left\{ q | q^T q = 1, q = [\eta_q\ ,\ \varepsilon_q^T]^T, \eta_q \in \mathbb{R}, \varepsilon_q \in \mathbb{R}^3 \right\} \tag{63}$$

$\omega_{\text{imu}} \in \mathbb{R}^3$ is the angular velocity vector measured by the gyros, $\hat{b}_{\text{gyro}} \in \mathbb{R}^3$ is the gyro bias, and $\omega_{in}^n = \omega_{ie}^n + \omega_{en}^n$ where $\omega_{ie}^n$ is the earth rate vector and $\omega_{en}^n$ is the angular velocity due to the movement of the ship over the earth. The latter component can be ignored for marine applications, while the former can be ignored if it is below the gyro noise level. Computation of $\omega_{ie}^n$ requires knowledge of true north. $T_{\text{gyro}} \in \mathbb{R}^{3\times3}$ is a diagonal time constant matrix, and $K_1 \in \mathbb{R}^{3\times3}$ and $K_2 \in \mathbb{R}^{3\times3}$ are diagonal matrices. Finally,

$$T_{\hat{q}}(\hat{q}) = \begin{bmatrix} -\hat{\varepsilon}_q^T \\ \hat{\eta}_q I + S(\hat{\varepsilon}_q) \end{bmatrix} \tag{64}$$

$$\Xi(\hat{q}) = \begin{bmatrix} -\hat{\varepsilon}_q^T \\ \hat{\eta}_q I - S(\hat{\varepsilon}_q) \end{bmatrix} \tag{65}$$

$\tilde{\varepsilon}_q$ and $\tilde{\eta}_q$ are components of the quaternion error $\tilde{q}$, which is computed from the estimated quaternion and a measurement quaternion derived from the accelerometer based attitude measurements. Since the accelerometer attitude measurement only needs to prevent the integrated gyro signal from drifting, the gains are usually chosen very small. This implies that horizontal accelerations have little influence on the roll and pitch measurements. Thus, these measurements can be used to compensate for the $g$-vector in the surge and sway acceleration measurements. Moreover, since the accelerometers are used for attitude computation, accelerometer bias will not influence the surge and sway measurements. Gravity compensation is carried out as follows:

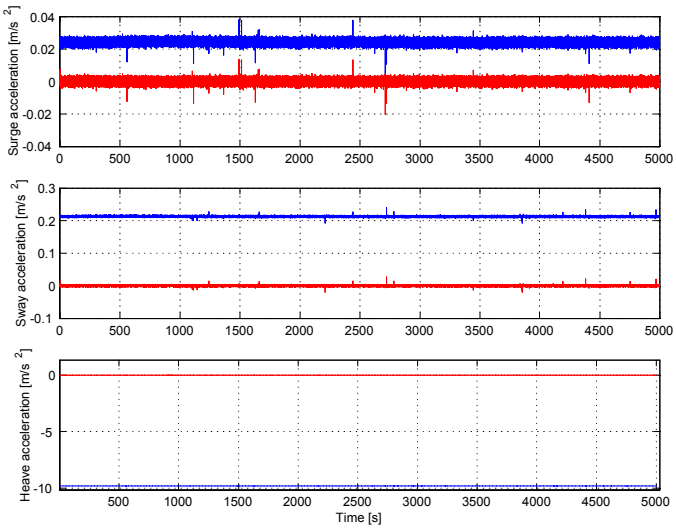


Figure 2: Measured and g-compensated accelerations. The noise level is about 120 $\mu g$ ($1\sigma$), and the offset after compensation is a few $\mu g$ on all three axes.

$$\begin{bmatrix} \dot{u} \\ \dot{v} \\ \dot{w} \end{bmatrix} = f_{\text{imu}} + \begin{bmatrix} -\sin\theta \\ \cos\theta\sin\phi \\ \cos\theta\cos\phi \end{bmatrix} g \tag{66}$$

where $g$ can be calculated with great accuracy if the latitude is approximately known. Figure 2 shows the measured and $g$-compensated acceleration in a static test.

## 6 Experiments

The experiment was carried out with "Cybership II", a 1:70 replica of an offshore supply vessel with overall length $L_{OA} = 1.255$ meters, see Figure 3.

Based on the principle of certainty of equivalence, an observer-feedback PID-like tracking controller

Figure 3: Cybership II

on the form

$$\dot{\xi} = \hat{\eta} - \eta_d \quad (67)$$

$$\tau = -K_i R^T(\hat{\psi})\xi - K_p R^T(\hat{\psi})(\hat{\eta} - \eta_d) - K_d(\hat{\nu} - \nu_d) \quad (68)$$

was used to keep the boat on the position $\eta_d = [-0.3, 0, 0]^T$, $\nu_d = 0$. The controller and the thrust allocation algorithm is described and analyzed in [6].

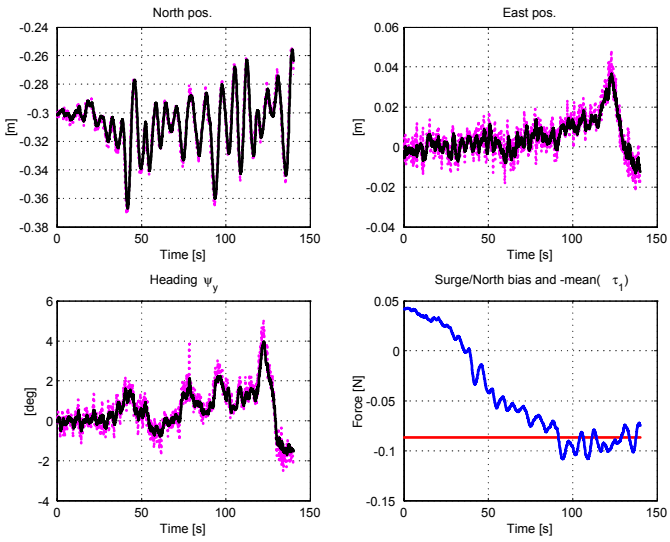


Figure 4: Top left, measured (dotted) and LF estimated North position. Top right, measured (dotted) and LF estimated East position. Bottom left, measured (dotted) and LF estimated heading. Bottom right, estimated bias and mean of applied thrust thrust $\tau_1$.

From $t \approx 20$ seconds and onwards, the model ship

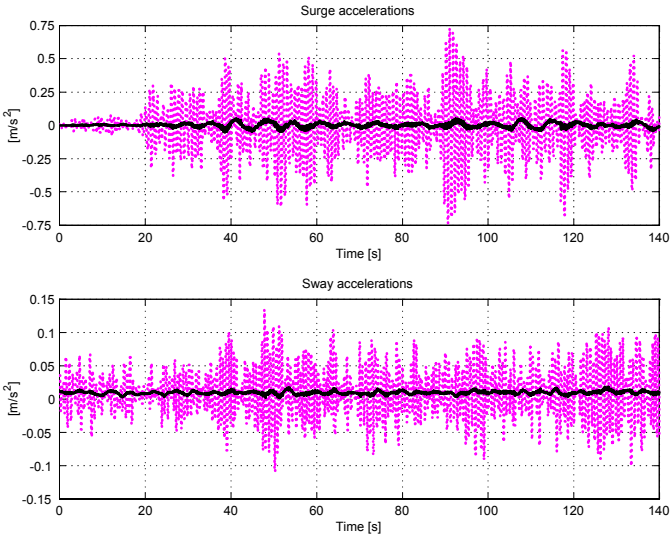


Figure 5: $g$-compensated surge and sway accelerations. Measurements (dotted) and LF estimates (solid).

was exposed to JONSWAP-distributed irregular head waves. The peak period and significant wave height were set to $T_s = 0.75$ and $H_{1/3} = 0.02$ meters respectively.

Time series plots of the measured (dotted magenta) positions and their respective LF estimates are reproduced in Figure 4 together with the observer's surge bias estimate. Notice that the surge bias converges towards the controller's I-term, that is the mean of applied surge propeller force $\tau_1$. A large wave slammed into the vessel at $t \approx 115$ generating a temporary drift off in East and heading because the vessel had a small offset angle at the time of the impact. The slow oscillations are due to nonlinear wave effects and not to the first order induced motion. Figure 5 shows $g$-compensated measurements of the surge and sway accelerations. Here, the wave frequency motion (first order wave loads) dominate the picture. But as the empiric transfer functions (Figure 6) of the measured signals and the state derivatives show, for low frequencies the estimated LF-accelerations are excellent, because they follow the measured signals at frequencies below $f = 0.1$ Hz. As required, frequency components around the wave frequency peak $f = 1/T_s = 1.33$ Hz

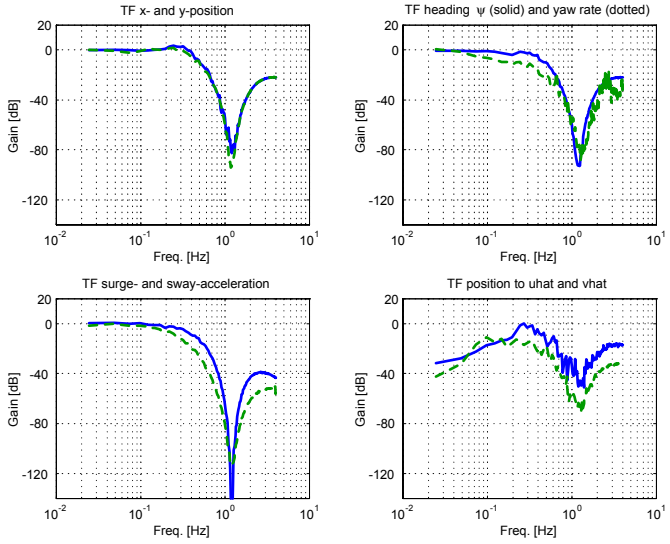


Figure 6: Top left, TF from measured North (solid) and East (dotted) position to their respective LF estimates. Top right, TF from measured heading (solid) and yaw rate (dotted) to LF estimates. Bottom left, TF from measured surge (solid) and sway acceleration to LF estimates. Bottom left, TF from North position to surge velocity (solid) and from East to sway (dotted).

have been successfully attenuated.

## 7 Concluding Remarks

A simple model based state estimator for surface vessels with wave filtering capabilities has been proposed and analyzed along with an intuitive tuning procedure. For bounded yaw rate, the observer error dynamics was shown to be exponentially stable. Inertial measurements, that is linear accelerations and yaw rate, were included in the filter to improve performance. Due to the acceleration measurement ambiguity, a $g$-compensation system had to be derived in order to remove gravity components from the linear acceleration terms.

Experimental results with a model ship performing a DP operation as it was exposed to incoming irregular waves illustrated the performance of the filter. Empirically calculated frequency responses between available measurements and estimated low frequency positions, velocites and accelerations documented that the desired notch filtering of first order wave induced motion was achieved.

## References

[1] A. B. Aalbers, R. F. Tap, and J. A. Pinkster. An application of dynamic positioning control using wave feed forward. *Int. Journal of Robust and Nonlinear Control*, 11:1207–1237, 2001.

[2] J. G. Balchen, N. A. Jenssen, and S. Sælid. Dynamic positioning using Kalman filtering and optimal control theory. In *IFAC/IFIP Symposium on Automation in Offshore Oil Field Operation*, pages 183–186, Amsterdam, Holland, 1976.

[3] T. I. Fossen. *Guidance and Control of Ocean Vehicles*. John Wiley & Sons, 1994.

[4] T. I. Fossen and J. P. Strand. Passive nonlinear observer design for ships using Lyapunov methods: Experimental results with a supply vessel. *Automatica*, 35(1):3–16, January 1999.

[5] K.-P. Lindegaard and T. I. Fossen. A model based wave filter for surface vessels using position, velocity and partial acceleration feedback. In *Proc. of the 40th IEEE Conf. on Decision and Control*, Orlando, FL, 2001.

[6] K.-P. Lindegaard and T. I. Fossen. Fuel efficient rudder and propeller control allocation for marine craft: Experiments with a model ship. *IEEE Trans. on Control Systems Technology*, 2002. Submitted February 20th, 2002.

[7] B. Vik and T. I. Fossen. Nonlinear observer design for integration of GPS and inertial navigation systems. In *Proc. of the 40th IEEE Conf. on Decision and Control*, Orlando, FL, 2001.